

# Demonstration that 1-*trans*-epoxysuccinyl-L-leucylamido-(4-guanidino)butane (E-64) is one of the most effective low $M_r$ inhibitors of trypsin-catalysed hydrolysis. Characterization by kinetic analysis and by energy minimization and molecular dynamics simulation of the E-64– $\beta$ -trypsin complex

Suneal K. SREEDHARAN\*, Chandra VERMA†, Leo S. D. CAVES†, Simon M. BROCKLEHURST‡, Saheer E. GHARBIAS, Haroun N. SHAH§ and Keith BROCKLEHURST\*||

\*Laboratory of Structural and Mechanistic Enzymology, Department of Biochemistry, Queen Mary and Westfield College, University of London, Mile End Road, London E1 4NS, U.K., †Protein Structure Research Group, Department of Chemistry, University of York, Heslington, York YO1 5DD, U.K., ‡Oxford Centre for Molecular Sciences, Department of Biochemistry, University of Oxford, South Parks Road, Oxford OX1 3QU, U.K., §Department of Microbiology, Eastman Dental Institute, University of London, Gray's Inn Road, London WC1X 8LD, U.K.

1-*trans*-Epoxy succinyl-L-leucylamido(4-guanidino)butane (E-64) was shown to inhibit  $\beta$ -trypsin by a reversible competitive mechanism; this contrasts with the widely held view that E-64 is a class-specific inhibitor of the cysteine proteinases and reports in the literature that it does not inhibit a number of other enzymes including, notably, trypsin. The  $K_i$  value ( $3 \times 10^{-5}$  M) determined by kinetic analysis of the hydrolysis of *N*<sup>ε</sup>-benzoyl-L-arginine 4-nitroanilide in Tris/HCl buffer, pH 7.4, at 25 °C,  $I = 0.1$ , catalysed by  $\beta$ -trypsin is comparable with those for the inhibition of trypsin by benzamidine and 4-aminobenzamidine, which are widely regarded as the most effective low  $M_r$  inhibitors of this enzyme. Computer modelling of the  $\beta$ -trypsin–E-64 adsorptive complex, by energy minimization, molecular dynamics simulation and Poisson–Boltzmann electrostatic-potential calculations,

was used to define the probable binding mode of E-64; the ligand lies parallel to the active-centre cleft, anchored principally by the dominant electrostatic interaction of the guanidinium cation at one end of the E-64 molecule with the carboxylate anion of Asp-171 ( $\beta$ -trypsin numbering from Ile-1) in the  $S_1$ -subsite, and by the interaction of the carboxylate substituent on C-2 of the epoxide ring at the other end of the molecule with Lys-43; the epoxide ring of E-64 is remote from the catalytic site serine hydroxy group. The possibility that E-64 might bind to the cysteine proteinases clostripain (from *Clostridium histolyticum*) and  $\alpha$ -gingivain (one of the extracellular enzymes from *Porphyromonas gingivalis*) in a manner analogous to that deduced for the  $\beta$ -trypsin–E-64 complex is discussed.

## INTRODUCTION

1-*trans*-Epoxy succinyl-L-leucylamido(4-guanidino)butane (E-64) (reviewed in [1]) is generally considered to be a potent class-specific inhibitor of the cysteine proteinases. It has been shown to be unreactive towards low  $M_r$  mercaptans and reported to fail to inhibit some other types of enzyme including, notably, the serine proteinases trypsin, chymotrypsin, kallikrein, plasmin and elastase [2,3]. E-64 was isolated from cultures of *Aspergillus japonicus* [2] and its chemical synthesis reported [4]; it is now commercially available. E-64 comprises epoxysuccinyl, leucyl-amino and butylguanidinium moieties with a carboxylate anion at one end of the molecule and a guanidinium cation at the other end (see Figure 1).

Inhibition by E-64 of most of the cysteine proteinases studied to date is time-dependent and stoichiometric. Its reactions with papain (EC 3.4.22.2) and actinidin (EC 3.4.22.14) have been characterized particularly thoroughly by X-ray crystallography [5,6] and by molecular dynamics simulation [7]. Reaction involves nucleophilic attack by the catalytic site thiolate anion of the enzyme on the epoxide group of E-64, probably by an  $S_N2$  mechanism, with inversion of configuration at C-2 (the carbon atom of the epoxide ring bearing the carboxylate substituent, see Figure 1) to produce the ring-opened product with a hydroxy group on C-3 (Figure 2). It is noteworthy, however, that

inhibition by E-64 of at least two cysteine proteinases does not occur by time-dependent covalent modification. We reported that  $\alpha$ -gingivain, one of the cysteine proteinases from *Porphyromonas gingivalis* [8–10], is inhibited ‘instantaneously’ by E-64 by a reversible competitive mechanism [11]. We also confirmed the earlier brief report [3] that E-64 acts as a reversible competitive inhibitor of clostripain (EC 3.4.22.8) the cysteine proteinase from *Clostridium histolyticum*.

Interaction of proteinases with substrates and inhibitors is generally described using the S–P and S'–P' subsite concept and notation of Berger and Schechter [12]. The crystal structure, at 2.4 Å resolution, of the product of the covalent modification of Cys-25 of papain by E-64 [5] shows that a binding mode involving the S'-subsites (those that bind the leaving group of a peptide substrate, i.e. residues on the C-terminal side of the scissile bond) proposed previously [3] is incorrect. In fact E-64 binds to the S-subsites, in a manner rather similar to that reported for the product of alkylation of Cys-25 by benzyloxycarbonyl-Phe-Ala chloromethyl ketone [13]. In E-64-modified papain, the Leu side-chain of the quasi-E-64 moiety is located at the entrance to the hydrophobic pocket of the  $S_2$ -subsite. The butylguanidinium cation appears to occupy a position similar to that of the benzyloxy group in papain alkylated by the chloromethyl ketone and, additionally, makes hydrogen-bonds with the hydroxy groups of Tyr-61 and Tyr-67 of the enzyme. The major features

Abbreviations used: E-64, 1-*trans*-epoxysuccinyl-L-leucylamido(4-guanidino)butane; E-64c, 1-*trans*-epoxysuccinyl-L-leucylamido-3-methylbutane; Bz-L-Arg-4NA, *N*<sup>ε</sup>-benzoyl-L-arginine 4-nitroanilide; a.b.N.R., adopted-basis Newton Raphson; m.d., molecular dynamics; s.d., steepest descent.

|| To whom correspondence should be addressed

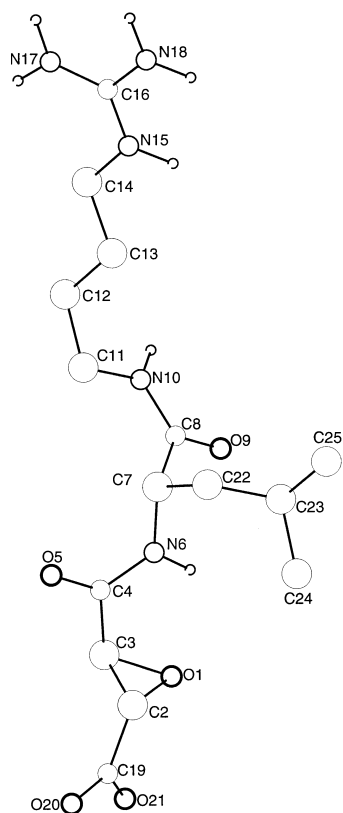


**Figure 1** The structure of E-64

The conformation shown is that obtaining in the crystal structure of the complex of E-64 with papain [5]; the coordinates were kindly supplied by C. P. Huber) and is in the conformation used for the initial docking into the active centre of  $\beta$ -trypsin. The structural features that are particularly noteworthy in the context of the present paper are the butyl guanidinium cation at one end of the molecule and the carboxylate anion at the other end; there are seven hydrogen-bond donor sites (deriving from NH and  $\text{NH}_2$  groups) and ten acceptor sites (deriving from five oxygen atoms).

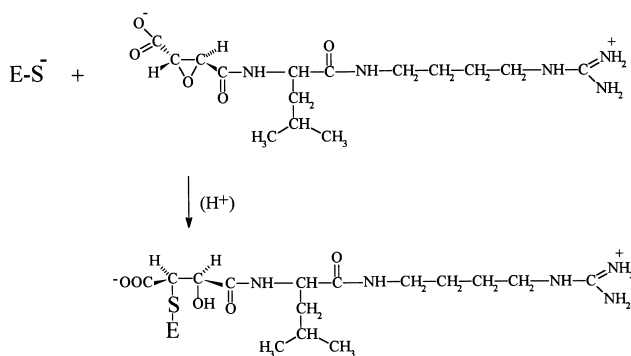


**Figure 2** Reaction of E-64 with the catalytic site thiol group of cysteine proteinases typified by papain

Reaction occurs by nucleophilic attack of the thiolate anion ( $\text{E-S}^-$ ) on the epoxide group of E-64, probably by an  $\text{S}_{\text{N}}2$  mechanism, with inversion of configuration at C-2 (the carbon atom of the epoxide ring bearing the carboxylate substituent) to produce the ring-opened product with a hydroxy group on C-3. E-64 does not react with low  $M_r$  mercaptans and it may be a requirement that the catalytic site environments provide hydrogen-bonding to the ring oxygen atom to enhance its leaving-group ability (see the Introduction for comment on reactions of E-64 with oxyanions and with HI).

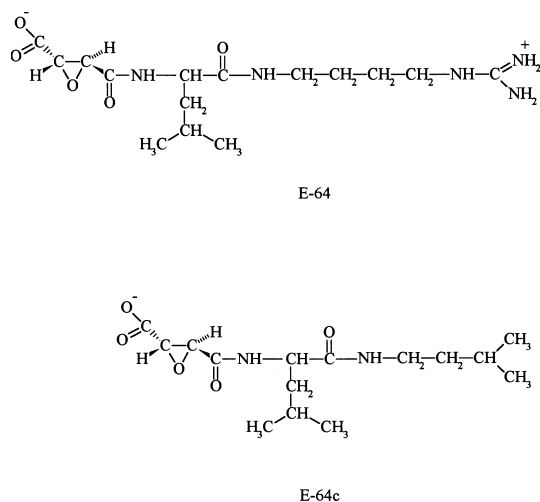


**Figure 3** Comparison of the chemical formulae of E-64 and E-64c

In E-64c the cationic guanidino group of E-64 is replaced by an electrically neutral aliphatic side-chain. Thus E-64c would be predicted not to be an inhibitor of enzymes where the key binding interaction of E-64 involves the guanidinium cation.

of the crystal structure [5] are consistent with the conclusions of the molecular dynamics simulation [7]. The crystal structure, at 1.86 Å resolution, of the product of the reaction of actinidin with E-64 [6] is, for the most part, closely similar to that of the analogous papain derivative [5]. There is, however, much less interaction of the butylguanidinium cation with actinidin than with papain.

Binding modes in complexes of E-64 with both papain and actinidin provide alignment of C-2 of the epoxide ring with the catalytic site thiolate anion. One explanation for the failure of E-64 to alkylate the catalytic site thiol groups of  $\alpha$ -gingivain and clostripain is that a different binding mode obtains in complexes of E-64 with these enzymes, which fails to present the electrophilic epoxide group to the catalytic site thiol groups in an appropriate mode, even though binding in the active-centre region is suggested by the observed competitive inhibition. A binding mode inappropriate for chemical modification might be grossly different from those found for papain and actinidin, such that the epoxide ring is remote from the catalytic site thiolate anion, or alternatively, might differ in a more subtle way. Epoxides do not alkylate low  $M_r$  thiolate anions. This suggests that, in reactions with thiolate anions, the alkoxide leaving group requires assistance by acid catalysis, which might be provided by hydrogen-bond donation in some cysteine proteinase catalytic sites, but perhaps not in others. An illustration of such a relationship between nucleophilicity and nucleofugacity is that epoxides can alkylate hard nucleophiles such as alkoxides and hydroxide ion, but also alkylate the soft nucleophile, iodide anion, when acid catalysis is available, as in reactions of HI (see e.g. [14]). The high specificity exerted by both clostripain and  $\alpha$ -gingivain for substrates and inhibitors with Arg at  $\text{P}_1$ , and their high affinity for Sepharose-Arg [15,16], suggests that a key feature of the binding of E-64 to these enzymes, whose structures have not yet been reported, might involve electrostatic interaction of the butylguanidinium cation in a putative anionic  $\text{S}_1$ -subsite. This might provide a binding mode grossly different from those observed with papain and actinidin. Support for a key  $\text{P}_1$ - $\text{S}_1$  interaction is provided by the failure of 1-*trans*-epoxysuccinyl-L-leucylamido-

3-methylbutane (E-64c; Figure 3) to inhibit both clostripain and  $\alpha$ -gingivain [3,10,17].

The possibility that E-64 might bind to sites in proteins with high affinity for alkylguanidinium cations led us to re-examine the surprising assertions reported in the literature [2,3] that E-64 does not inhibit trypsin, a view that appears to have gained wide acceptance (see e.g. [1]), despite the well-known affinity of its  $S_1$ -subsite for cationic ligands (see e.g. [18,19]). We here report kinetic evidence that both  $\alpha$ -trypsin and  $\beta$ -trypsin (jointly designated EC 3.4.21.4) are indeed inhibited by E-64, the latter at least in a reversible competitive manner. This modifies the widely held view that E-64 is a specific inhibitor for cysteine proteinases. Computer modelling suggests a minimum-energy binding mode involving two electrostatic interactions, one involving the butyl-guanidinium cation of E-64 with the carboxylate anion of Asp-177 in the  $S_1$ -subsite and the other involving the carboxylate substituent on C-2 of the epoxide ring of E-64 with the  $\epsilon$ -alkylammonium ion of Lys-43.

## MATERIALS AND METHODS

### Materials

E-64, E-64c,  $N^{\alpha}$ -benzoyl-L-arginine 4-nitroanilide (Bz-L-Arg-4NA), 4-nitrophenyl-4-guanidinobenzoate hydrochloride,  $N^{\alpha}$ -benzoyl-L-tyrosine ethyl ester and twice crystallized, lyophilized bovine trypsin and chymotrypsin were obtained from Sigma (Poole, Dorset, U.K.). A pre-packed Mono S HR 5/5 FPLC column was supplied by Pharmacia (GB) Ltd.

### Fractionation of trypsin

Trypsin was fractionated by ion-exchange chromatography by adapting the method described in [20] for use with FPLC equipment. A solution of the commercial trypsin (2 ml of 10 mg/ml) in 0.1 M-Tris/HCl buffer, pH 7.1, containing 0.02 M  $\text{CaCl}_2$  was applied to the Mono S column via a Whatman 0.2  $\mu\text{m}$  filter, and the protein components were eluted using 0.1 M Tris/HCl buffer, pH 7.1, containing 1.0 M NaCl and 0.02 M  $\text{CaCl}_2$ . The elution was monitored at 280 nm and fractions were collected and assayed for catalytic activity towards Bz-L-Arg-4NA as described below, except that a substrate concentration of 500  $\mu\text{M}$  was used. The fractions comprising each of the two major protein ( $A_{280}$ ) peaks possessing catalytic activity were pooled to provide stock solutions of  $\alpha$ -trypsin (the first peak to be eluted) and  $\beta$ -trypsin (the second peak to be eluted). These were each brought to pH 3.0 with 1 mM HCl and stored at 4 °C.

The concentration of trypsin protein was determined by measurement of  $A_{280}$  and quantified by using  $\epsilon_{280} = 3.0 \times 10^4 \text{ M}^{-1} \cdot \text{cm}^{-1}$ , calculated from  $A^{1\%} = 12.9$  [21] and  $M_r = 2.34 \times 10^4$  [22]. The same value of  $\epsilon_{280}$  was assumed for both forms of trypsin. Active-site titration (see [23] for a review) was carried out by using 4-nitrophenyl-4'-guanidino benzoate as described in [24]. The concentration of  $\alpha$ -chymotrypsin protein was determined by measurement of  $A_{282}$  and quantified by using  $\epsilon_{282} = 5.0 \times 10^4 \text{ M}^{-1} \cdot \text{cm}^{-1}$  [22].

### Kinetic measurements

The release of 4-nitroaniline resulting from the hydrolysis of Bz-L-Arg-4NA catalysed by  $\alpha$ -trypsin (5.9  $\mu\text{M}$ ) and  $\beta$ -trypsin (4.9  $\mu\text{M}$ ) in Tris/HCl buffer, pH 7.4, at 25.0 °C and  $I = 0.1$  was monitored by measurement of the increase in  $A_{410}$  in a Cary 1 spectrophotometer and quantified by using  $\Delta\epsilon_{410} = 8.80 \times 10^3$

$\text{M}^{-1} \cdot \text{cm}^{-1}$  as described for ficin-catalysed hydrolysis [25]. To determine whether the postulated inhibition of trypsins by E-64 is 'time-dependent' or 'instantaneous', the catalytic activity of the enzymes towards Bz-L-Arg-4NA (150  $\mu\text{M}$ ) was measured after nine time-intervals of 10–60 min over a 3 h period in the absence and the presence of E-64 (50  $\mu\text{M}$ , 100  $\mu\text{M}$  and 300  $\mu\text{M}$ ).

Inhibition occurred within 1 min, was dependent on [E-64] and the extent of the inhibition did not change further over the 3 h period. Analogous experiments using E-64c at concentrations up to 1 mM failed to produce inhibition of the trypsin-catalysed hydrolysis.

The hydrolysis of  $N^{\alpha}$ -benzoyl-L-tyrosine ethyl ester catalysed by  $\alpha$ -chymotrypsin in 0.1 M Tris/HCl buffer, pH 7.8, at 25 °C was monitored at 256 nm as described in [26] in the absence and in the presence of up to 1 mM E-64 and, separately, up to 1 mM E-64c. Having established the inhibition of the trypsins by E-64 to be instantaneous, the mode of inhibition was further defined for  $\beta$ -trypsin, the variant for which a crystal structure is available, by measuring values of the initial rate, using 4.9  $\mu\text{M}$   $\beta$ -trypsin over a range of values of the substrate concentration [S] (96–671  $\mu\text{M}$ ) in the absence ( $v_o$ ) and in the presence ( $v_i$ ) of 50  $\mu\text{M}$  E64.

### Computer modelling of the structure of bovine $\beta$ -trypsin and its complex with E-64

The crystal structure of bovine  $\beta$ -trypsin at 1.5 Å resolution (Brookhaven protein database, entry 1 tld; [27]) was used as the basis for the modelling procedures. This protein consists of 223 amino acid residues (six fewer than trypsinogen), 1 calcium ion, 1 sulphate ion (deleted in the models) and 25 crystallographic water molecules. The structure of E-64 (Figure 1) was taken from the crystal structure of the papain-E-64 complex ([5]; coordinates kindly supplied by C. P. Huber, Department of Biochemistry, University of Ottawa, Canada).

The protein was modelled using the extended-atom param 19/top 19 CHARMM force field [28], which employs an explicit representation of all non-hydrogen atoms and polar hydrogen atoms. The latter were added using the HBUILD functionality [29] of CHARMM. Charges were assigned using the standard CHARMM parameter sets [30,31]. Non-bonded interactions were calculated using a Coulomb potential, with the solvent screening being effected by use of a distance-dependent dielectric [32,33]. This approach was found to give satisfactory results in the study of the interactions between trypsin and benzamide [34]. In the present work, a constant dielectric constant of 1.0 was used when bulk solvent was modelled explicitly. Solvent water was represented using a modified form of the TIP3 model described in [35]. The non-bonded interactions were truncated by a shifted potential [28] with a 12 Å cut-off [36]. Electrostatic interactions between atoms separated by three covalent bonds were scaled to 50 % of their value. Minimizations were carried out using the steepest descent (s.d.) and adopted-basis Newton Raphson (a.b.N.R.) algorithms [28]. Molecular dynamics (m.d.) simulations were started by assigning random velocities (corresponding to a mean temperature of 300 K) to the atoms from a Gaussian distribution. The SHAKE algorithm [37,38] was used to constrain all bond lengths to their equilibrium values with a relative tolerance of  $10^{-6}$ , thus enabling a time step of 0.002 ps to be used for the integrations of the equations of motion. The systems were coupled to an external bath at a constant temperature of 300 K with a coupling constant ( $\tau_r$ ) of 1.0 ps [39]. Non-bonded lists were updated every 0.05 ps using a 14 Å cut-off. The multiple-copy simulation methodology [40] was used to

sample multiple ligand conformations [41]. In this methodology, which allows for simultaneous inclusion of several ligand conformations in a single simulation, the ligands do not interact with each other but only with the rest of the system. The interaction of each ligand with the rest of the system is scaled down by a factor that is proportional to the number of ligands used. The REPLICA functionality of CHARMM was used to partition the system into primary (protein/ion/solvent) and replicated (ligand) subsystems. All calculations were performed on a network of Silicon Graphics workstations. QUANTA (MSI, Waltham, U.S.A.) and IDRAW were used for visualizations and graphics.

The initial (crystal) structure of  $\beta$ -trypsin was assumed to contain electrically neutral His side-chains and fully charged Asp, Glu, Lys and Arg side-chains. The position of the N-H moiety of each His-imidazole group was determined by protonating each of the two N atoms in turn, evaluating the energy of the system and selecting the side-chain structure with the lower energy. This provided maximum hydrogen-bonding opportunities. Similarly, the conformations of the side-chains of the Asn and Gln residues were examined by interchanging the positions of the oxygen atoms and  $\text{NH}_2$  groups. The conformations with the lowest overall energies and maximum hydrogen-bonding opportunities with surrounding atoms were used.

The crystal structure of  $\beta$ -trypsin, thus modified, was solvated by overlaying a pre-equilibrated sphere of bulk water molecules, such that a shell of water around the enzyme, at least 6 Å thick, was retained in the model. The hydrogen atoms of the added water were rebuilt in the field of the static protein using HBUILD. The system was constrained in the positions of all non-hydrogen atoms by a harmonic force constant of  $1.0 \text{ kcal} \cdot \text{mol}^{-1} \cdot \text{Å}^{-2}$  and subjected to minimizations using 200 steps of s.d. and 500 steps of a.b.N.R. Then E-64, in the conformation obtaining in its complex with papain, was docked into the active-centre cleft of  $\beta$ -trypsin such that the two  $\text{NH}_2$  groups of its guanidinium cation were positioned near to the carboxylate anion at the end of the  $S_1$ -subsite [Asp-189 using the numbering system of the crystal structure, which is Asp-171 of the  $\beta$ -trypsin sequence (see the Results and Discussion section)]. Similar binding geometries are observed in crystal structures of  $\beta$ -trypsin complexed with other cationic ligands, e.g. benzamidine (Brookhaven entry 3ptb).

Interchange of the binding positions of the two  $\text{NH}_2$  groups of E-64 leads to two conformations of the bound ligand, one in which E-64 protrudes into solvent (conformer I) and the other in which it lies almost parallel to the active centre cleft (conformer II, in which initial clashes with the protein were removed by varying torsional angles, guided by visual inspection using QUANTA). At this stage, a search for local variation of each of the two initial conformations was made within the static environment of the protein. Following energy minimization (100 steps of s.d. followed by 500 steps of a.b.N.R.) the E-64 ligand was allowed to explore the local potential-energy surface via a high-temperature (1000 K) m.d. simulation [42] for 100 ps. The resulting trajectory was sampled every 1 ps and the transient conformations of E-64 were minimized (200 steps of s.d. and a.b.N.R.) until a uniform value of the gradient ( $10^{-3} \text{ kcal} \cdot \text{mol}^{-1} \cdot \text{Å}^{-1}$ ) was reached. Ten lowest energy conformations were taken from the studies of both initial conformers of E-64 (see above) and used for further modelling. This included both m.d. simulations on each structure individually solvated, and REPLICA m.d. simulations on 50 conformers (representing the last 50 ps in each study) of E-64 in the active centre of  $\beta$ -trypsin. Each of these structures was hydrated within a 25 Å radius from the centroid of the catalytic site serine residue (Ser-177 of the  $\beta$ -trypsin sequence, see the Results and Discussion section).

## RESULTS AND DISCUSSION

### The bovine trypsins: amino acid residue numbering systems

Bovine trypsinogen is a 229-residue single-chain protein with six intra-chain disulphide cross-links and an N-terminal Val residue (see [43]). The native form of trypsin ( $\beta$ -trypsin, also a single-chain protein) is formed during trypsinogen activation by hydrolytic removal of a hexapeptide (Val-Asp-Asp-Asp-Asp-Lys) to produce a new N-terminus (Ile). In some reports (e.g. [44]) the trypsinogen sequence numbering system is retained for  $\beta$ -trypsin, in which case the N-terminal Ile is referred to not as Ile-1 but as Ile-7, the catalytic triad as Ser-183, His-46 and Asp-90 and the anionic residue in the  $S_1$ -subsite as Asp-177. In many other papers, including the report of the 1.5 Å crystal structure [27], residues are numbered by analogy with the chymotrypsinogen numbering system [45] such that the N-terminal Ile is Ile-16, the catalytic triad is the familiar Ser-195, His-57 and Asp-102 and the  $S_1$ -anionic site is Asp-189. In the present paper, the modified structural model of  $\beta$ -trypsin and its complex with E-64 is described in terms of the actual sequence of  $\beta$ -trypsin (i.e. with Ile-1, Ser-177, His-40 and Asp-84 as the catalytic triad and Asp-171 in the  $S_1$ -subsite) with the corresponding numbers taken from the crystal structure given in parenthesis in some instances.

Commercial trypsin products have been found to contain three distinct molecular forms of catalytically active protein, all with the same  $M_r$  value ( $\alpha$ ,  $\beta$  and  $\Psi$  trypsins, the latter known also as pseudo-trypsin [20,44,46]). Hydrolytic cleavage of  $\beta$ -trypsin at the Lys-131–Ser-132 bond (trypsinogen numbering) produces  $\alpha$ -trypsin, comprising two chains held together by disulphide bonds. Hydrolytic cleavage of  $\alpha$ -trypsin at the Lys-176–Asp-177 bond (trypsinogen numbering) produces  $\Psi$ -trypsin, comprising three chains held together by disulphide bonds. In the present work, only  $\alpha$ -trypsin and  $\beta$ -trypsin were found in significant amounts in Sigma trypsin, and both of these forms were found to be inhibited by E-64 (see below).

### Investigation of the possibility of inhibiting $\alpha$ - and $\beta$ -trypsins and $\alpha$ -chymotrypsin by E-64 and E-64c

Initial studies on these potential inhibitions, as described in the Materials and methods section, demonstrated that both trypsin variants are inhibited instantaneously by E-64, but no inhibition could be detected either of the trypsin-catalysed hydrolysis by E-64c or of the  $\alpha$ -chymotrypsin-catalysed hydrolysis by E-64 or E-64c.

### Kinetic analysis of the inhibition of $\beta$ -trypsin by E-64

Detailed kinetic studies were carried out on  $\beta$ -trypsin, the trypsin variant for which three-dimensional structural information is available. Plots of initial rate, in the absence ( $v_0$ ) and in the presence ( $v_i$ ) of E-64 (50  $\mu\text{M}$ ) versus [S] for the hydrolysis of Bz-L-Arg-4NA catalysed by  $\beta$ -trypsin are shown in Figure 4. The data adhere well to the Michaelis–Menten equation. The continuous lines were constructed using the values of  $V_{\text{max}}^0$  and  $K_m^0$  (for the reaction in the absence of E-64) and of  $V_{\text{max}}^i$  and  $K_m^i$  (for the inhibited reaction) obtained by fitting the data to the hyperbolic form of the rate equation using the weighted non-linear regression program in SIGMAPLOT. These values of the four parameters ( $V_{\text{max}}^0 = 3.23 \times 10^{-7} \pm 0.11 \times 10^{-7} \text{ M} \cdot \text{s}^{-1}$ ;  $K_m^0 = 397 \pm 31 \mu\text{M}$ ;  $V_{\text{max}}^i = 3.68 \times 10^{-7} \pm 0.62 \times 10^{-7} \text{ M} \cdot \text{s}^{-1}$ ;  $K_m^i = 1140 \pm 270 \mu\text{M}$ ) demonstrate the competitive nature of the inhibition. The values were used to construct lines through the data in double-reciprocal plots [47] (not shown). The intersection of the two lines essentially on the ordinate axis, reflecting the closely

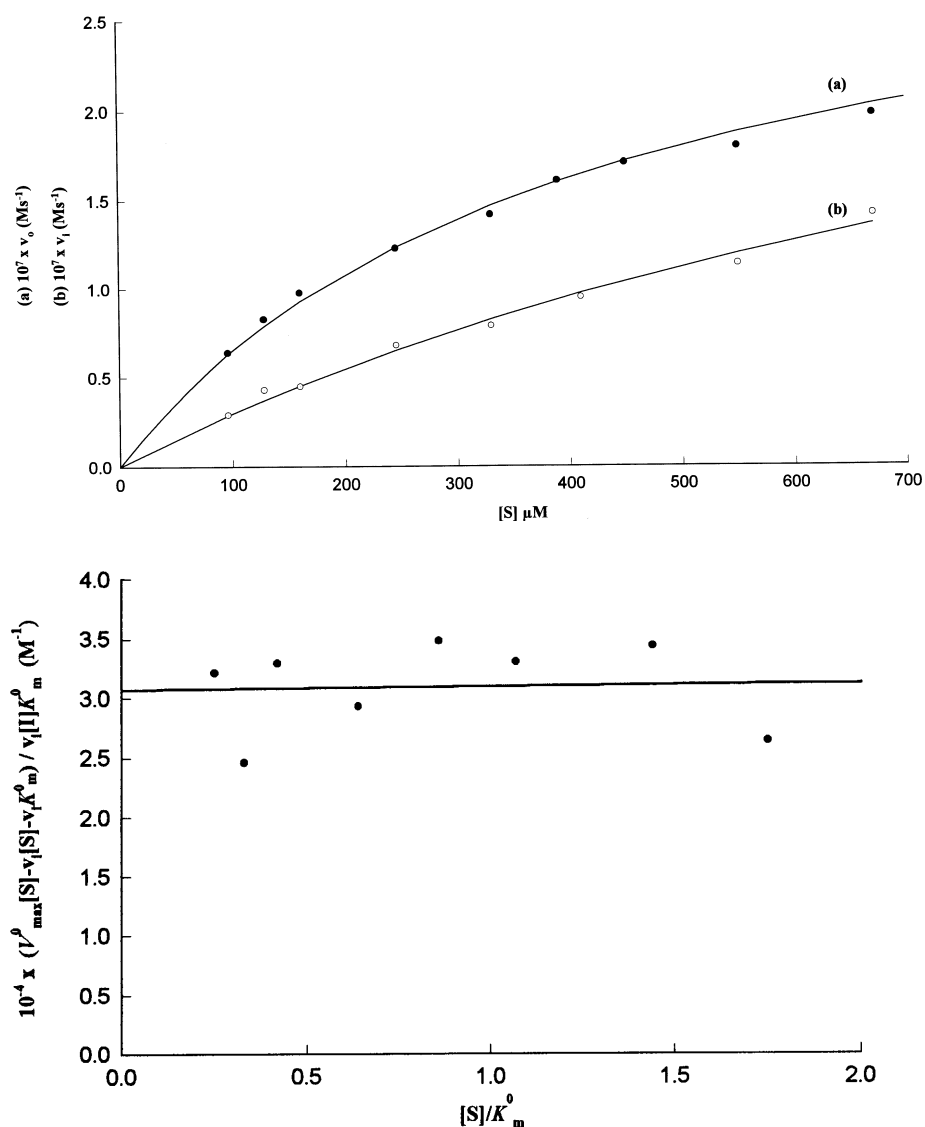


**Figure 4** Top: dependence of the initial rate (a) in the absence ( $v_0$ ) and (b) in the presence ( $v_i$ ) of 50  $\mu\text{M}$  E-64 on  $[\text{S}]$  for the hydrolysis of Bz-L-Arg 4NA catalysed by 4.9  $\mu\text{M}$   $\beta$ -trypsin in Tris/HCl buffer, pH 7.4, at 25  $^\circ\text{C}$  and  $I = 0.1$ : demonstration of the competitive nature of the inhibition by E-64 and evaluation of the  $K_i$  value. Bottom: use of the  $V_{\text{max}}^0$  version of the optimized combination plot [50] to demonstrate the competitive nature of the inhibition of  $\beta$ -trypsin by E-64 and to evaluate the  $K_i$  value

Top: the points are experimental data pairs and the continuous lines were constructed using the values  $V_{\text{max}}^0 = 3.23 \times 10^{-7} (\pm 0.11 \times 10^{-7}) \text{ M} \cdot \text{s}^{-1}$  and  $K_m^0 = 397 (\pm 31) \mu\text{M}$  (for the reaction in the absence of E-64) in curve a, and the values of  $V_{\text{max}}^i = 3.68 \times 10^{-7} (\pm 0.62 \times 10^{-7}) \text{ M} \cdot \text{s}^{-1}$  and  $K_m^i = 1140 (\pm 270) \mu\text{M}$  (for the inhibited reaction) in curve b, obtained by fitting the data to the hyperbolic form of the Michaelis–Menten equation using the weighted non-linear regression program in SIGMAPLOT. Bottom: the plot was constructed by using the data shown in the top part of the figure and eqn. (6) of the text with  $n = 1$ , i.e.  $(V_{\text{max}}^0[\text{S}] - v_i[\text{S}] - v_i K_m^0) / v_i [I] K_m^0 = 1/K_i$ . The regression line, essentially parallel with the abscissa, i.e. independent of  $[\text{S}]/K_m^0$ , demonstrates the competitive nature of the inhibition and provides the value of  $K_i$  as 33  $\mu\text{M}$ .

similar values of  $V_{\text{max}}^0$  and  $V_{\text{max}}^i$ , provides the classical illustration of the competitive nature of the inhibition. As is well known, the value of  $K_i$ , the dissociation equilibrium constant of the  $\beta$ -trypsin–E-64 complex, may be computed by using eqn. (2), a transform of the expression for  $K_m^i$  for competitive inhibition [eqn (1)].

$$K_m^i = K_m^0 (1 + [I]/K_i) \quad (1)$$

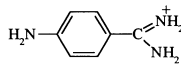
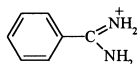
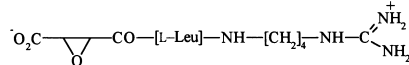
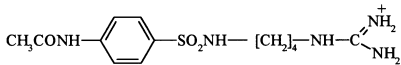
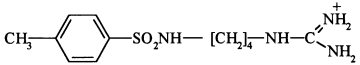
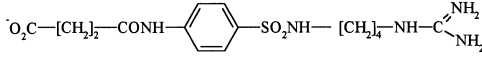
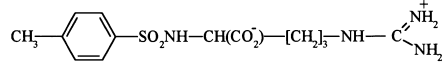
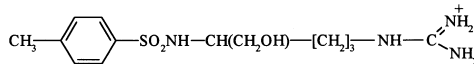
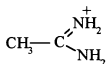
$$K_i = K_m^0 [I] / (K_m^i - K_m^0) \quad (2)$$

Using this method, the value of  $K_i$  for the inhibition of  $\beta$ -trypsin by E-64, under the conditions given in the Materials and methods section, was calculated to be 27  $\mu\text{M}$ . It has been conventional to

obtain more accurate values of  $K_i$  either by using the well-known Dixon plot [48] in which  $1/v_i$  is plotted against  $[I]$  for different values of  $[\text{S}]$  or by plotting the slopes of the double-reciprocal plots ( $1/v_i$  versus  $1/[\text{S}]$ ) against  $[I]$ . Both procedures require the concentrations of substrate and inhibitor to be varied separately and, thus, are laborious. By using the function  $(v_0 - v_i)/v_i$ , however, it is possible to transform rate equations so that a single line accommodates all data points regardless of the inhibitor and substrate concentrations [49]. Recently, Chan [50] has introduced new versions (combination plots) of the Hunter and Downs plot [49], which are linear, of characteristic appearance for each of the competitive, non-competitive, uncompetitive and linear mixed types of inhibition, and provide an efficient method of obtaining

**Table 1** The effectiveness of E-64 and some analogues as competitive inhibitors of trypsin-catalysed hydrolysis

Values of  $K_i$  have been rounded to one significant figure. References and reaction conditions: (a) Mares-Guia and Shaw [19]; substrate, the Bz-L-Arg-4NA component of the racemic mixture, pH 8.15, 15°C; the kinetic treatment takes into account the presence of the D-isomer of the substrate, which is another competitive inhibitor; (b) present work; substrate Bz-L-Arg-4NA, pH 7.4, 25°C,  $I = 0.1$ ; (c) Rule and Lorand [18]; substrate N<sup>α</sup>-acetyl-L-leucine 4-nitrophenylester, pH 8.0,  $I \approx 0.34$ , 3.3% (v/v) acetone and 13.3% (v/v) isopropanol.

Inhibitor	$K_i$ (M)	Reference and reaction conditions
4-aminobenzamidine	$8 \times 10^{-6}$	(a)
		
benzamidine	$2 \times 10^{-5}$	(a)
		
E-64	$3 \times 10^{-5}$	(b)
		
4-acetamidophenylsulphonylagmatine	$2 \times 10^{-4}$	(c)
		
tosylagmatine	$5 \times 10^{-4}$	(c)
		
4-succinamidophenylsulphonylagmatine	$5 \times 10^{-4}$	(c)
		
N <sup>α</sup> -tosyl-L-argininine	$5 \times 10^{-3}$	(c)
		
N <sup>α</sup> -tosyl-L-argininol	$1 \times 10^{-2}$	(c)
		
acetamidine	$4 \times 10^{-2}$	(a)
		

good estimates of  $K_i$  values, particularly when the version that makes use of  $V_{\max}$  rather than  $v_o$  values is used (see below).

Chan [50] derived eqns. (3)–(5) for competitive, non-competitive and uncompetitive inhibition respectively, in which  $y = (1 + [S]/K_m^o)(v_o - v_i)/v_i$  [I].

$$y = 1/K_i \quad (3)$$

$$y = (1 + [S]/K_m^o)/K_i \quad (4)$$

$$y = [S]/K_m^o K_i \quad (5)$$

When  $y$  is plotted against  $[S]/K_m^o$ , only in the case of competitive inhibition is  $y$  invariant as  $[S]/K_m^o$  varies. The regression line is parallel with the abscissa and  $K_i$  is calculated from  $y = 1/K_i$  [eqn. (3)]. Statistical fluctuation of individual  $v_o$  values contributes to scatter in the data and this is decreased by using functions equivalent to  $y$  but expressed in terms of  $V_{\max}$  instead of  $v_o$  [eqn. (6)], where  $n = 1$  for competitive inhibition and  $1 + [S]/K_m^o$  and  $[S]/K_m^o$  for non-competitive and uncompetitive inhibition respectively].

$$(V_{\max}^o [S] - v_i [S] - v_i K_m^o)/v_i [I] K_m^o = n/K_i \quad (6)$$

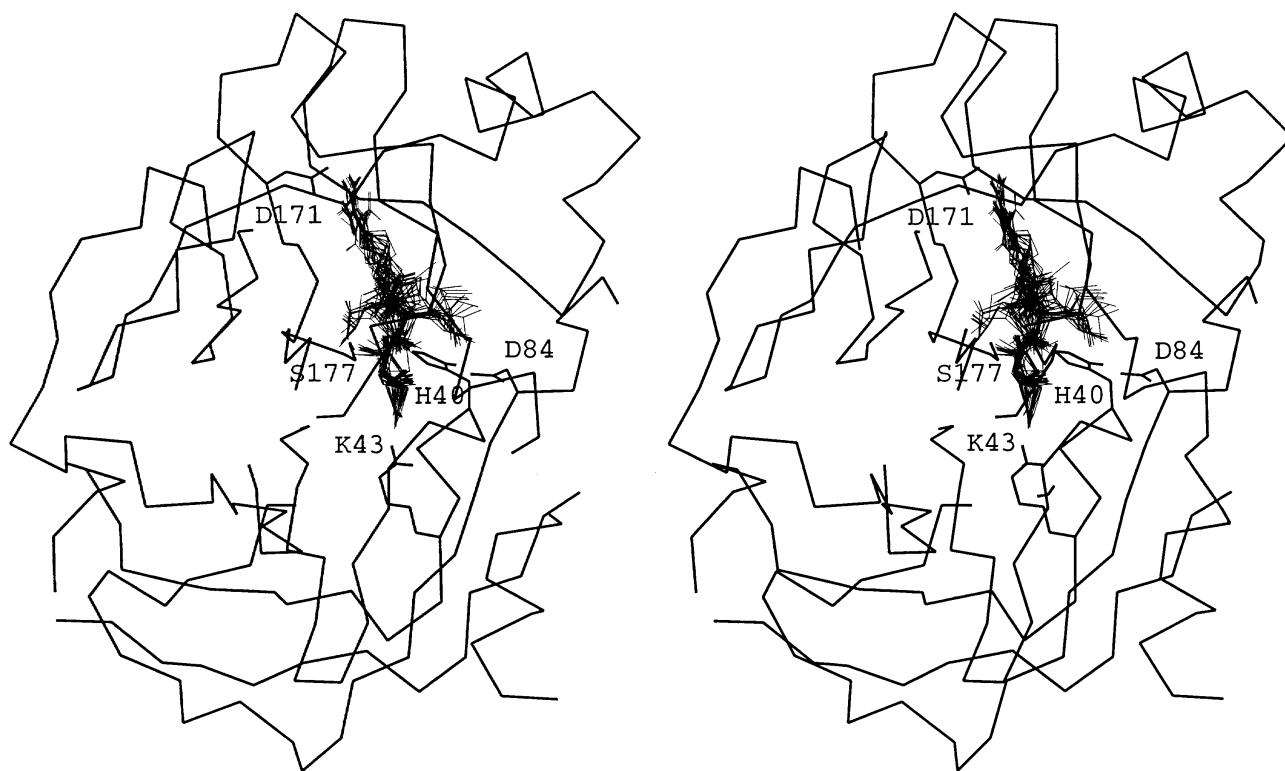


**Figure 5** Stereo view of 50 superimposed conformations of E-64 in the active-centre cleft of  $\beta$ -trypsin to illustrate the conformational variability of the ligand

The structures are from the multiple-copy REPLICAs calculations. Only the  $C^\alpha$  atoms, the non-hydrogen atoms of the catalytic triad (H40, D84, S177) (one-letter amino acid code) and the electrostatic binding sites (K43, D171) of the protein are shown in addition to the E-64 conformations. Following minimization of E-64, the minimum energy conformations generated from both of the initial conformers (I and II, see the text) cluster in similar conformations in which the ligand lies parallel with the active-centre cleft.

The expression on the left-hand side of eqn. (6) is readily shown to be identical with  $\gamma$  by substituting the right-hand side of the Michaelis–Menten equation, i.e.  $V_{\max}^o[S]/(K_m^o + [S])$ , for  $v_o$  in the expression for  $\gamma$  and simplifying. A combination plot relating to eqn. (6) for the inhibition of  $\beta$ -trypsin-catalysed hydrolysis by E-64 is shown in Figure 4 (bottom). The regression line through the data, essentially parallel with the abscissa, demonstrates the competitive nature of the inhibition and provides the value of  $K_i$  as 33  $\mu\text{M}$ .

#### Comparison of the characteristics of E-64 and some guanidinium and amidinium analogues as competitive inhibitors of trypsin-catalysed hydrolysis

The values of  $K_i$  for the analogues (see Table 1) are taken from the literature [18, 19]. The experiments were performed before the fractionation of commercial trypsin into  $\alpha$ - and  $\beta$ -trypsins had been reported in [20]. Nevertheless, the reactions catalysed by commercial trypsin preparations obeyed the Michaelis–Menten equation. This, together with our preliminary characterization of the competitive inhibition of  $\alpha$ -trypsin by E-64, where the  $K_i$  value does not differ from that for the analogous inhibition of  $\beta$ -trypsin by more than a factor of 2, suggests that the  $K_i$  values in Table 1 (albeit determined under a variety of experimental conditions) provide a useful guide to the way in which inhibitory effectiveness varies with the structure of the inhibitor. It is noteworthy that the value of  $K_i$  for E-64 is similar to those for benzamidine and 4-aminobenzamidine (all approx.  $10^{-5}$  M) which are usually regarded as the most effective low  $M_i$  inhibitors

of trypsin-catalysed hydrolysis. These three compounds are about ten times more effective as inhibitors than the three arylsulphonylagmatines shown in Table 1 ( $K_i = 2 \times 10^{-4}$ – $5 \times 10^{-4}$  M) including 4-succinylamidophenylsulphonylagmatine, which like E-64, contains a carboxylate anion at the end of the molecule remote from the butylguanidinium cation.  $N^{\omega}$ -tosyl-L-arginine ( $K_i = 5 \times 10^{-3}$  M) and  $N^{\omega}$ -tosyl-L-argininol ( $K_i = 1 \times 10^{-2}$  M), in which the butylguanidinium moiety of the agmatine-derived inhibitors is shortened to a propylguanidinium moiety, are even less effective inhibitors, comparable to the simplest analogue, acetamidine ( $K_i = 4 \times 10^{-2}$  M).

#### Investigation of the $\beta$ -trypsin–E-64 binding mode by computer modelling

Optimization of the hydrogen-bonding potentials around the side-chains of Asn and Gln residues of  $\beta$ -trypsin resulted in the interchange of the side-chain oxygen atoms and the side-chain  $\text{NH}_2$  groups of three Asn residues and six Gln residues. This produced a decrease in the non-bonded energy of the system by approx.  $150 \text{ kcal} \cdot \text{mol}^{-1}$ , 85% of which originated from electrostatic effects. The substantial stabilization of the conformation thus produced, emphasizes the necessity to examine the orientations of polar side-chains in crystal structures prior to minimization. Solvation of the protein and minimization as described in the Materials and methods section resulted in only small changes in the crystal structure (a root mean square deviation of 0.2 Å over all atoms, with changes of the order of 0.5 Å localized at atoms exposed to solvent). Two of the 25 water

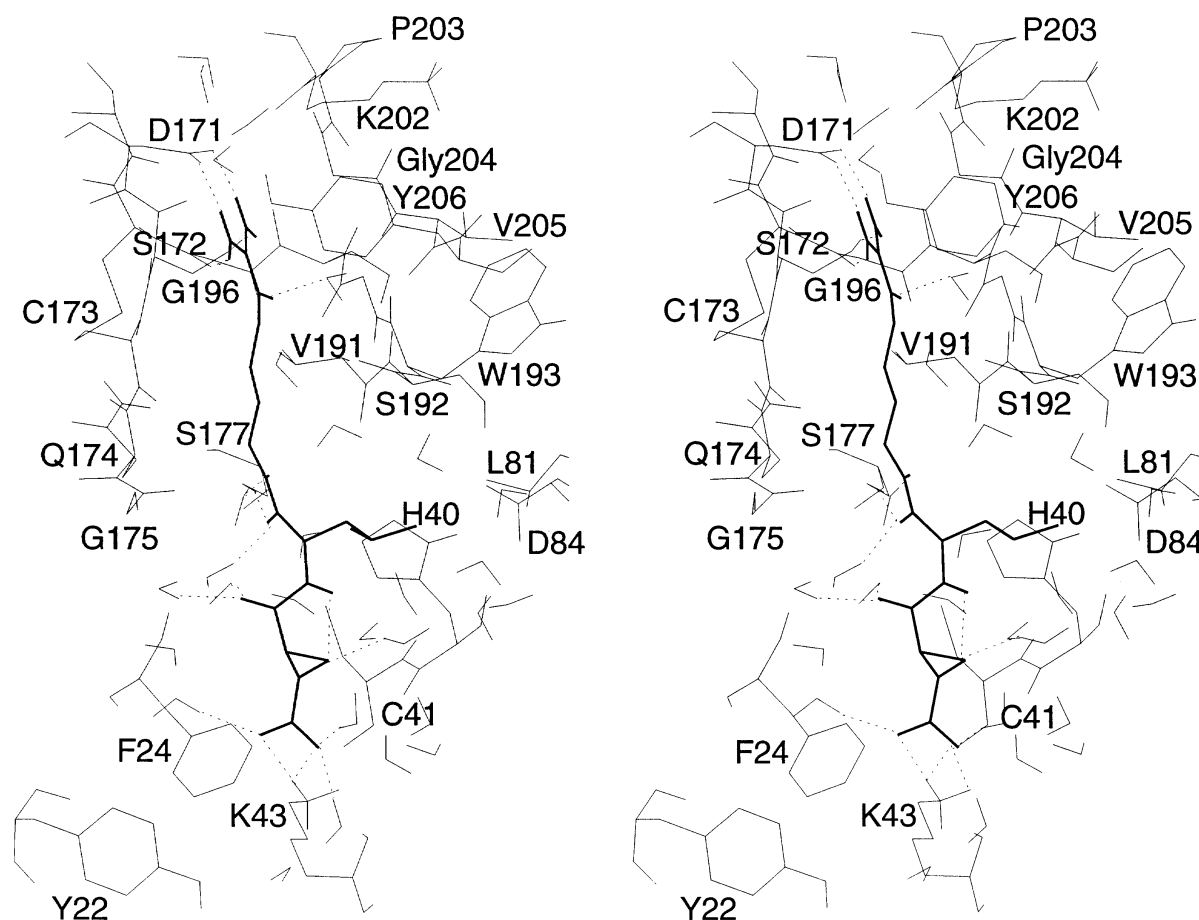


**Figure 6** A representative minimum energy conformation of E-64 bound to the active centre of  $\beta$ -trypsin

The transient structure was taken from an m.d. simulation and energy minimized. E-64 is shown as a thick line, the protein as thin lines and the hydrogen bonds and electrostatic interactions (involving D177 and K43) (one-letter amino acid code) that stabilize the modelled binding mode as broken lines.

molecules had to be deleted consequent upon rigid docking of E-64 into the active centre, due to the positioning of the guanidinium moiety near to Asp-171 (Asp-189) to prevent overlap of the water molecules with E-64. The E-64 molecule contains seven hydrogen-bond donor sites (deriving from NH and NH<sub>2</sub> groups) and ten acceptor sites (deriving from five oxygen atoms) (see Figure 1). Clearly the strongest binding modes would satisfy all of the hydrogen-bonding potential of E-64. The active-centre cleft of  $\beta$ -trypsin is lined with several polar sites, which could accept or donate hydrogen bonds [27,51]. Rigid-body docking calculations using QUANTA, which optimize the rotational and translational degrees of freedom of the whole ligand, while keeping the rest of the system fixed, and evaluation of the energy of interaction, suggest conformer II to be more stable than conformer I by up to 200 kcal·mol<sup>-1</sup>. In the former, E-64 lies almost parallel to the active-centre cleft whereas in the latter it protrudes into solvent. The additional stabilization in conformer II originates mainly from stronger interactions between (a) the guanidinium cation of E-64 (NH<sub>2</sub> groups at positions 17 and 18 in Figure 1) and the carboxylate anion of Asp-171 (Asp-189) in the S<sub>1</sub>-subsite and (b) the carboxylate substituent of E-64 on C-2 of the epoxide (O20 and O21 in Figure 1) and both Lys-43 and Tyr-22. Other contributions to the stabilization of conformer II derive from interactions between polar groups on E-64 and those lining the active-centre cleft. Following minimization of E-64, the minimum

energy conformations generated from both of the initial conformers (I and II) cluster in similar conformations in which E-64 lies parallel to the active-centre cleft (Figure 5). In these conformations, the two electrostatic interactions described above are augmented by hydrogen-bonding interactions involving Ser-172, Cys-173, Asn-174, Gly-175, Ser-177, Ser-192, Gly-194, Ser-195, Gly-196 and several water molecules. The minimum energy structure resulting from initial conformer II is more stable than that resulting from initial conformer I by approx. 7 kcal·mol<sup>-1</sup>. While both ends of the E-64 molecule are strongly localized by the two electrostatic interactions, there is considerable conformational flexibility in the middle of the molecule and positional variability in the leucyl side-chain. Hydrogen-bond analyses of the m.d. simulations show that N-17/N-18 of E-64 are held by electrostatic interaction to the side-chain of Asp-171 and additionally make strong hydrogen-bonds with the backbone carbonyl oxygen atoms of Ser-172 and Gly-196 and with the side-chain of Ser-172. Further stabilization is provided by a crystallographic water molecule. Stabilization of N-15 of E-64 is through the side-chain of Ser-172 and a crystallographic water molecule. At the other end of the ligand, O-20 and O-21 are stabilized by electrostatic interaction with Lys-43 and strong interactions with several bulk water molecules. The side-chain of Ser-177 is involved in stabilizing O-5 and O-9, but because of the large conformational variability in this part of E-64, these two



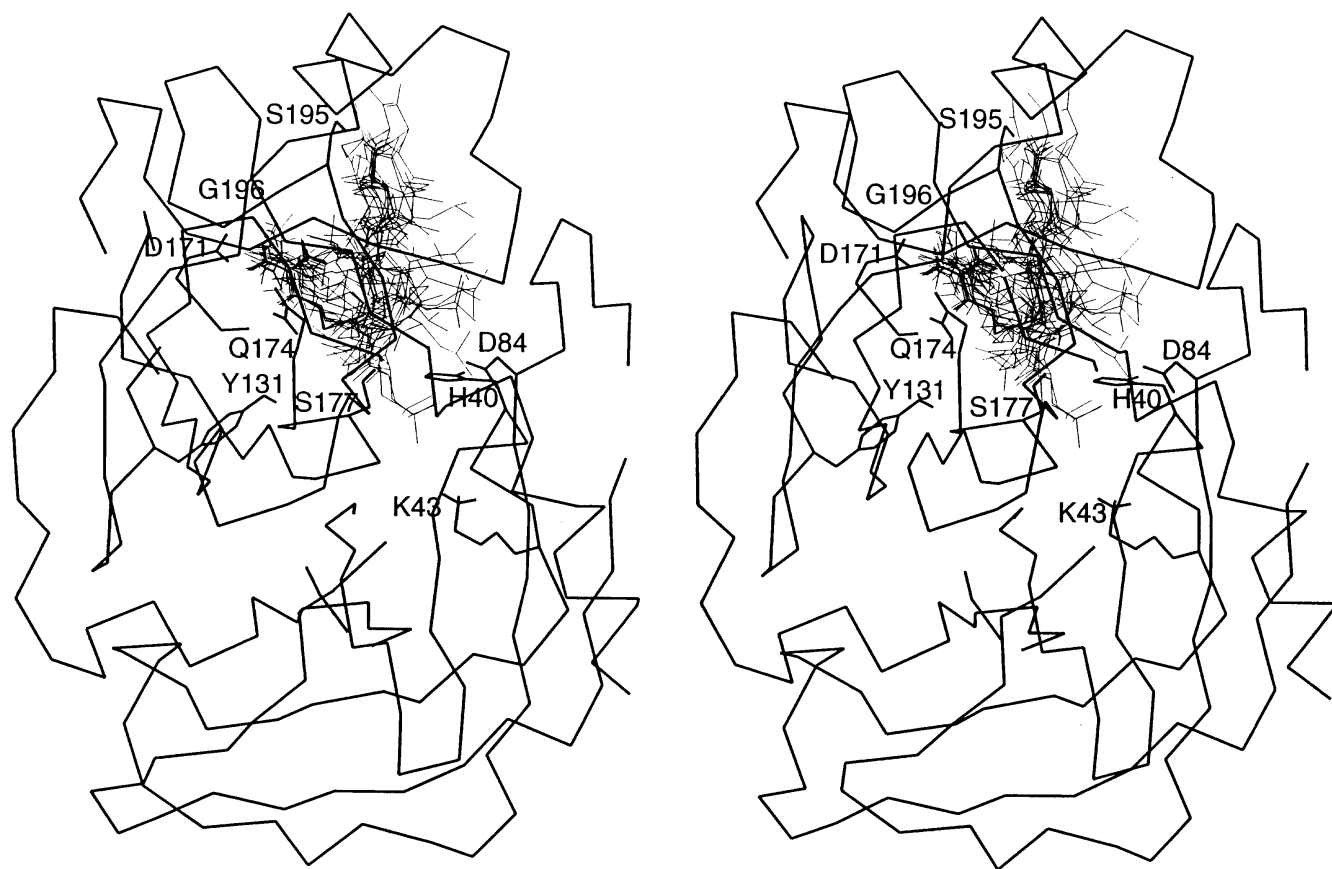


**Figure 7** The modes of binding of E-64 to  $\beta$ -trypsin in the absence of the charge on Lys-43

When the charge on Lys-43 is switched off the clustering of the ligand conformations shown in Figure 5 is no longer present. Instead, several different clusters exist with E-64 stabilized in several conformational substates by several small lobes of positive potential in or near the mouth of the active-centre cleft. The dominance of the electrostatic interaction of the guanidinium cation of E-64 with Asp-171 in the  $S_1$ -subsite is shown to be preserved in the absence of the other electrostatic interaction (with Lys-43) at the other end of the E-64 molecule.

sites are well hydrated. A hydrogen-bond between O-1 and N-6 exists for about 85% of the simulation, although O-1 is also well hydrated. Root mean square fluctuations of the atoms of the ligand during the m.d. simulations show that, while the fluctuations in E-64 are smaller than 0.5 Å towards the guanidinium end (as a result of its being packed in the  $S_1$ -pocket), the rest of the molecule undergoes 50–100% larger fluctuations; the C-7–C-25 region undergoes the largest motion with amplitudes ranging between 0.6 and 2.0 Å.

Figure 5 is a stereo view of 50 superimposed conformations of E-64 bound in the active-centre cleft of  $\beta$ -trypsin to illustrate the conformational variability of the ligand. The ligand structures were obtained from multiple-copy REPLICAs calculations. Figure 6 shows a representative minimum energy conformation taken from an m.d. simulation and minimized. In terms of electrostatic effects, the active-centre cleft of  $\beta$ -trypsin is bounded by the partially buried, negatively charged, side-chain of Asp-171 on one side and by the exposed positively charged side-chain of Lys-43 on the other. Poisson–Boltzmann electrostatic potential calculations using the University of Houston Brownian Dynamics program (version 5.1; [52,53]) reveal a very diffuse negative potential ( $-1.0 \text{ kcal} \cdot \text{mol}^{-1}$ ) around Asp-171, which probably drives the binding of the guanidinium cation to the  $S_1$ -binding pocket. By contrast, the positive potential in the region around Lys-43 is localized. Although there are other lobes of positive potential around the mouth of the active-centre cleft, the binding

of the guanidinium cation in the  $S_1$ -subsite restricts the disposition of the rest of the E-64 ligand, including the carboxylate end. As a result of this restriction, the electrostatic interaction of the carboxylate anion of E-64 and Lys-43 contributes most to the stabilization in the allowed conformational substates and leads to the clusters of binding modes shown in Figure 5. When the same procedure of locating the binding mode of E-64 is carried out with the charge on the side-chain of Lys-43 switched off, the clustering shown in Figure 5 is no longer present (see Figure 7). Instead, several different clusters exist with E-64 stabilized in several conformational substates by several lobes of positive potential in or near the mouth of the active-centre cleft. Figure 7 serves to emphasise the dominance of the electrostatic interaction of the guanidinium cation of E-64 with Asp-171 in the  $S_1$ -subsite in the binding of E-64 to  $\beta$ -trypsin, and the necessary role of the other electrostatic interaction (with Lys-43) in defining the binding mode illustrated in Figures 5 and 6.

### Concluding comments

In the present work, a combination of kinetic analysis and computer modelling has demonstrated that E-64 is one of the most effective low  $M_r$  competitive inhibitors of trypsin-catalysed hydrolysis so far discovered, and suggests a binding mode involving two electrostatic interactions, one at each end of the E-64 molecule, such that the epoxide ring of the inhibitor is remote

from the catalytic site of the enzyme. If a similar binding mode obtains for the interaction of E-64 with the cysteine proteinases clostripain and  $\alpha$ -gingivain, that would explain why these enzymes are inhibited competitively by E-64 and not by time-dependent covalent modification, which occurs with some other cysteine proteinases such as papain, actinidin and cathepsins B, H and L (see [3]). We have concluded previously that the widely applied designation of at least one of the extracellular proteinases of *P. gingivalis* ( $\alpha$ -gingivain, see [8,9]) as 'trypsin-like' is inappropriate, because this enzyme does not resemble trypsin either in its catalytic site or in its specificity characteristics in view of its high selectivity for P<sub>1</sub>-Arg as against P<sub>1</sub>-Lys [11]. This selectivity is not shared by trypsin [54,55], although mutagenesis of Asp-177 (189) and/or Ser-178 (190) can produce selectivity [55,56]. The fact that E-64 has now been shown to inhibit trypsin (as well as  $\alpha$ -gingivain) by a competitive mechanism does not change the conclusion that  $\alpha$ -gingivain is not 'trypsin-like' in any substantive way involving either its substrate specificity or its catalytic site structure. The extent of the similarity between trypsin,  $\alpha$ -gingivain and clostripain may be restricted to an anionic S<sub>1</sub>-subsite able to engage a guanidinium cation in a dominant electrostatic interaction. Differences in S<sub>1</sub>-subsite geometries could account for the variation in selectivity for P<sub>1</sub>-Arg as against P<sub>1</sub>-Lys in substrate recognition among the two cysteine proteinases and the serine proteinase, trypsin.

K.B. and H.N.S. thank MRC and BBSRC for project grants providing Pre-doctoral and Post-doctoral Research Assistantships for S.K.S. S.M.B. thanks Professor I. D. Campbell, FRS, for support and is supported by the MRC Research Fellowship Scheme; The Oxford Centre for Molecular Sciences is supported by BBSRC, MRC and EPSRC. C.V. thanks the Wellcome Trust for a Research Fellowship. We thank C. P. Huber for supplying the co-ordinates of E-64.

## REFERENCES

- Shaw, E. (1990) *Adv. Enzymol.* **63**, 271–347
- Hanada, K., Tamai, M., Yamagishi, M., Ohmura, S., Sawada, J. and Tanaka, I. (1978) *Agric. Biol. Chem.* **42**, 523–528
- Barrett, A. J., Kembhavi, A. A., Brown, M. A., Kirschke, H., Knight, C. G., Tamai, M. and Hanada, K. (1982) *Biochem. J.* **201**, 189–198
- Hanada, K., Tamai, M., Ohmura, S., Sawada, J., Seki, T. and Tanaka, I. (1978) *Agric. Biol. Chem.* **42**, 529–536
- Varughese, K. I., Ahmed, F. R., Carey, P. R., Hasnain, S., Huber, C. P. and Storer, A. C. (1989) *Biochemistry* **28**, 1330–1332
- Varughese, K. I., Sum Y., Cromwell, D., Hasnain, S. and Xuong, N. (1992) *Biochemistry* **31**, 5172–5176
- Yamamoto, D., Ohishi, H., Ishida, T., Inoue, M., Sumiya, S. and Kitamura, K. (1990) *Chem. Pharm. Bull.* **38**, 2339–2343
- Shah, H. N., Gharbia, S. E., Kowlessur, D., Wilkie, E. and Brocklehurst, K. (1990) *Biochem. Soc. Trans.* **18**, 578–579
- Shah, H. N., Gharbia, S. E., Kowlessur, D., Wilkie, E. and Brocklehurst, K. (1991) *Microbiol. Ecol. Health Dis.* **4**, 319–328
- Sreedharan, S. K. (1995) Ph.D. Thesis, University of London
- Sreedharan, S. K., Patel, H., Smith, S., Gharbia, S. E., Shah, H. N. and Brocklehurst, K. (1993) *Biochem. Soc. Trans.* **21**, 218S
- Berger, A. and Schechter, I. (1970). *Philos. Trans. R. Soc. London, Ser B* **257**, 249–264
- Drenth, J., Kalk, K. H. and Swen, H. M. (1976) *Biochemistry* **15**, 3731–3738
- Isaacs, N. S. (1987) *Physical Organic Chemistry*, pp. 210–254, Longmans Scientific and Technical, London
- Emöd, I. and Keil, B. (1977) *FEBS Lett.* **77**, 51–56
- Pike, R., McGraw, W., Potempa, J. and Travis, J. (1994) *J. Biol. Chem.* **269**, 406–411
- Sreedharan, S. K., Shah, H. N. and Brocklehurst, K. (1994) *Biochem. Soc. Trans.* **22**, 212S
- Rule, N. G. and Lorand, L. (1964) *Biochim. Biophys. Acta* **81**, 130–135
- Mares-Guia, M. and Shaw, E. (1965) *J. Biol. Chem.* **240**, 1579–1585
- Schroeder, D. D. and Shaw, E. (1968) *J. Biol. Chem.* **243**, 2943–2949
- Shaw, E., Mares-Guia, M. and Cohen, W. (1965) *Biochemistry* **4**, 2219–2224
- Wilcox, P. E. (1970) *Methods Enzymol.* **19**, 64–108
- Brocklehurst, K. (1996) in *Enzymology Labfax* (Engel, P. C. ed.), pp. 1–87, Bios Scientific Publishers Ltd., Oxford and Academic Press Inc., San Diego
- Chase, Jr., T. and Shaw, E. (1969) *Biochemistry* **8**, 2212–2224
- Malthouse, J. P. G. and Brocklehurst, K. (1976) *Biochem. J.* **159**, 221–234
- Walsh, K. A. and Wilcox, P. E. (1970) *Methods Enzymol.* **XIX**, 31–41
- Bartunik, H. D., Summers, I. J. and Bartsch, H. H. (1989) *J. Mol. Biol.* **210**, 813–828
- Brooks, B. R., Bruccoleri, R. E., Olafson, B. D., States, D. J., Swaminathan, S. and Karplus, M. (1983) *J. Comput. Chem.* **4**, 187–217
- Brunger, A. and Karplus, M. (1988) *Protein Struct. Func. Genet.* **6**, 32–45
- Momany, F. A. and Rone, R. (1992) *J. Comput. Chem.* **13**, 888–900
- Tanner, J. J., Smith, P. E. and Krause, K. L. (1993) *Protein Sci.* **2**, 927–935
- Guenot, J. and Kollman, P. A. (1992) *Protein Sci.* **1**, 1185–1205
- Guenot, J. and Kollman, P. A. (1993) *J. Comput. Chem.* **14**, 295–311
- Luty, B. A., Wasserman, Z. R., Stouten, P. F. W., Hodge, C. N., Zacharias, M. and McCammon, J. A. (1995) *J. Comput. Chem.* **16**, 454–464
- Jorgensen, W. L., Chandrasekhar, J., Medura, J. D., Impey, R. W. and Klein, M. L. (1983) *J. Chem. Phys.* **79**, 926–935
- Lonchariach, R. J. and Brooks, B. R. (1989) *Protein Struct. Func. Genet.* **6**, 32–45
- Ryckaert, J. P., Ciccotti, G. and Berendsen, H. J. C. (1977) *J. Comput. Phys.* **23**, 327–341
- van Gunsteren, W. F. and Karplus, M. (1982) *Macromolecules* **15**, 1528–1544
- Berendsen, H. J. C., Potsma, P. M., van Gunsteren, W. F., Di Nola, A. and Haak, J. R. (1984) *J. Chem. Phys.* **81**, 3684–3690
- Elber, R. and Karplus, M. (1990) *J. Am. Chem. Soc.* **112**, 9161–9175
- Roitberg, A. and Elber, R. (1991) *J. Phys. Chem.* **95**, 9277–9287
- Bruccoleri, R. E. and Karplus, M. (1990) *Biopolymers* **29**, 1847–1862
- Keil, B. (1971) in *The Enzymes* (Boyer, P. B., ed), Vol. 3, pp. 249–275, Academic Press, New York and London
- Smith, R. L. and Shaw, E. (1969) *J. Biol. Chem.* **244**, 4704–4712
- Hartley, B. S., Brown, J. R., Kauffman, D. L. and Smillie, L. B. (1965) *Nature (London)* **207**, 1157–1159
- Foucault, G., Seydoux, F. and Yon, J. (1974) *Eur. J. Biochem.* **47**, 295–302
- Lineweaver, H. and Burk, D. (1934) *J. Am. Chem. Soc.* **56**, 658–666
- Dixon, M. (1953) *Biochem. J.* **55**, 170–171
- Hunter, A. and Downs, C. E. (1945) *J. Biol. Chem.* **157**, 427–446
- Chan, W. W.-C. (1995) *Biochem. J.* **311**, 981–985
- Soman, K., Yang, A.-S., Honig, B. and Fletterick, R. (1989) *Biochemistry* **28**, 9918–9926
- Davis, M. E., Madura, J. D., Sines, J., Luty, B. A., Allison, S. A. and McCammon, J. A. (1991) *Methods Enzymol.* **202**, 473–497
- Madura, J. D., Briggs, J. M., Wade, R. C., Davis, M. E., Luty, B. A., Ilin, A., Antosiewicz, J., Gilson, M. K., Bagheri, B., Scott L. R., McCammon, J. A. (1995) *Comput. Phys. Commun.* **91**, 57–95
- Cole, P. W., Murakami, K. and Inagami, T. (1971) *Biochemistry* **10**, 4246–4252
- Evnin, L. B., Vasques, J. R. and Craik, C. S. (1990) *Proc. Natl. Acad. Sci. U.S.A.* **87**, 6659–6663
- Perona, J. J., Tsu, A., McGrath, M. E., Craik, C. S. and Fletterick, R. J. (1993) *J. Mol. Biol.* **230**, 934–949